JOURNAL OF CATALYSIS 64, 38–50 (1980)

Tracer Studies of the Reaction Paths of the CO Oxidation over Polycrystalline Palladium and Rhodium

TATSUO MATSUSHIMA

Research Institute for Catalysis, Hokkaido University, Sapporo 060, Japan

Received October 22, 1979; revised February 13, 1980

The reaction path of the CO oxidation over polycrystalline palladium and rhodium was studied by a transient isotope tracer method. An isotopic composition of CO_2 produced transiently was monitored by mass spectrometry where the surface covered by given amounts of ^{13}CO and ^{12}CO was exposed to a gas mixture of ^{12}CO and O_2. The initial ratio of $^{13}CO_2$ to $^{12}CO_2$ in carbon dioxide produced was equal to that of ^{13}CO to ^{12}CO in carbon monoxide preadsorbed for all conditions studied. Carbon monoxide immediately prior to the oxidation was concluded to be in a chemisorption state, i.e., carbon dioxide is produced through the interaction between a CO ad-molecule and an oxygen ad-atom (a Langmuir–Hinshelwood process). No contribution from an Eley–Rideal process, namely, CO(phys. ad) + O(ad) → CO_2, was observed.

1. INTRODUCTION

The elementary CO_2 formation process involved in the CO oxidation over platinum metals is traditionally described by two models: an Eley–Rideal (ER) process, namely, CO(phys. ad) + O(chem. ad) → CO_2, and a Langmuir–Hinshelwood (LH) process, namely, CO(chem. ad) + O(chem. ad) → CO_2. A clear distinction between the processes on the basis of their rate expressions is, however, practically impossible, because the surface process for the CO_2 formation itself is so rapid that the overall CO_2 production is controlled by the adsorption of CO (*1–9*) or oxygen (*2, 4, 7, 10, 11*), depending on the experimental conditions. And further the rate of the CO_2 formation through the LH process is not simply proportional to the product of the coverages of CO and oxygen (*11–14*).

Recently Engel and Ertl (*15–17*) have determined the surface residence time for CO associated with the oxidation on Pd(111) using a modulated molecular beam technique. The magnitude and the temperature dependence are in agreement with the kinetic behavior of the LH process. Their analysis, however, was limited to a high temperature (>500 K) and was made on the basis of the rate expressions assumed. Their method can hardly be applied at low temperatures, because the steady CO_2 formation is too slow and further the rate expressions used have not been verified (*11–14*). On the other hand the transient isotope tracer method (*9, 18, 19*) is useful at low temperatures to distinguish between the ER and LH processes, since no assumption regarding the rate expressions for the constituent processes are required. The difference between the two processes exists in the state of the CO immediately prior to the oxidation. In the ER process CO behaves kinetically as if it directly encounters and reacts with an oxygen ad-atom from the gas phase, whereas in the other case CO is chemisorbed. The isotope carbon 13 can be used to distinguish adsorbed CO from gas-phase CO. In the experiments the catalyst surface is covered in advance by carbon monoxide labeled with carbon 13 and then treated with a mixture of oxygen and ordinary carbon monoxide. If the LH process is operative, the initial isotope ratio in the carbon dioxide produced should be equal to that in the carbon monoxide preadsorbed. On the other hand if the ER process is

0021-9517/80/070038-13$02.00/0

operative, no $^{13}CO_2$ should be produced. Over platinum (*9, 18*) and iridium (*19*) this tracer method was successfully applied and the LH process was concluded. In this paper, a clear distinction between the two processes will be given over palladium and rhodium by using this tracer method.

2. EXPERIMENTAL

The experimental apparatus and procedures were essentially the same as those reported previously (*9, 18, 19*). The system was a bakeable ultrahigh vacuum apparatus with a base pressure less than 3×10^{-7} Pa (1 Pa = 7.5×10^{-3} Torr). The catalyst—a polycrystalline Pd foil ($30 \times 5 \times 0.05$ mm) or Rh foil ($30 \times 8 \times 0.05$ mm)—could be heated resistively. Reactant gases, CO, O_2, ^{13}CO, $C^{18}O$ (carbon 12 and oxygen 16 are simply designated as C and O, respectively), and their mixtures were introduced independently through variable leak valves. Temperatures were monitored with a Pt–Pt/Rh thermocouple spot-welded on the catalyst. Prior to the experiments the catalyst was exposed to oxygen at a pressure of 1×10^{-4} Pa and a temperature of 900 K for several hours, and then flashed to 1000 K for Pd or to 1300 K for Rh under vacuum for a few tens of minutes. Several repetitions of this treatment have been shown to be sufficient to establish stable catalyst behavior. The surfaces of Pd and Rh foils pretreated in a similar way were analyzed by AES in a separate system. They were clean except for a trace of oxygen, which was not removed by CO exposure. All of these experiments utilize a hot-filament electron supply in the mass spectrometer. There was a significant background CO_2 formation on the filament, which was measured separately with the catalyst covered fully by CO at room temperature and subtracted from the measurements made under the same gas compositions.

3. RESULTS AND DISCUSSION

In the transient tracer experiments the catalyst is covered in advance by carbon monoxide labeled with carbon 13 and then treated with a mixture of oxygen and ordinary carbon monoxide. The isotopic composition of the CO_2 produced is monitored by mass spectrometry. In order to survey the conditions suitable for this tracer experiment, for example, temperatures at which significant CO_2 production and slow displacement of adsorbed isotopic carbon monoxide were observed, several preliminary experiments were conducted. The results on Pd were first summarized and then compared with those on Rh.

The isotopic mixing in carbon monoxide was examined by monitoring the mass 31 peak due to the production of $^{13}C^{18}O$ when both $^{13}C^{16}O$ and $^{12}C^{18}O$ were dosed. A small amount of $^{13}O^{18}O$ formation (less than 3% of the total carbon monoxide peak) was observed. It was negligibly small in the following tracer experiments.

3.1. Transient CO_2 Production over Palladium

3.1.a. General feature. The transient phenomena of the CO_2 production depended on the pressure and the composition of the dosed gas, the catalyst temperature, and the initial CO coverage, θ_{CO}^0. Figure 1 shows a typical transient CO_2 production on Pd induced at $\theta_{CO}^0 < 0.03$ and room temperature. The CO_2 partial pressure is proportional to the CO_2 production rate, since the reaction system was continuously pumped by an ion pump. The surface was exposed to a gas mixture of CO and O_2 ($CO/O_2 = 0.2$) at a total pressure of 0.7×10^{-4} Pa, while the CO_2, CO, and O_2 peaks were recorded. The total pressure was kept almost constant by monitoring the current of the ion pump. The CO_2 production maximized around 50 s after the onset of the transient production and decreased rapidly to the background level. The O_2 pressure remained almost constant, while the CO pressure built up around 150 s since the oxidation and the adsorption were finishing. The transient CO_2 production was completed in a shorter period than that on

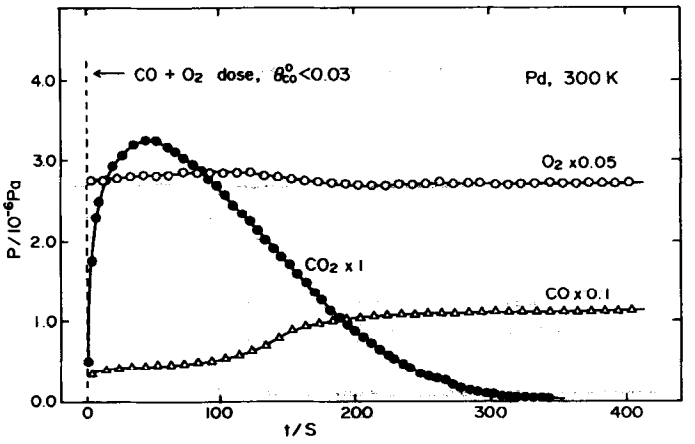

FIG. 1. Application of the (CO + O_2) pressure jump to induce a transient CO_2 production over Pd at 300 K. Variation of the partial pressures of CO, O_2, and CO_2 during a dosage of the mixture gas was shown. The apparent total pressure is 0.7×10^{-4} Pa.

Pt and the amount of CO_2 produced was less than a half of that on Pt under similar conditions (*9, 18*). This is attributed to rapid adsorption of CO on Pd (*1*).

3.1.b. Pressure dependence. The maximum rate in the transient CO_2 production was roughly proportional to the pressure of the dosed gas mixture of a fixed composition. The amount of CO_2 produced was almost independent of it. A typical example is shown in Fig. 2. Therefore, the transient isotope tracer method was applied under relatively low pressures because of the limitation of the instrument response time.

3.1.c. Temperature dependence. At relatively low temperatures, CO_2 was produced only transiently and the rate at a steady state was negligibly small. The amount of CO_2 produced increased with the temperature rise. At high temperature (>375 K) the CO_2 production increased sharply up to a steady state, but did not show a maximum. These phenomena may be attributed to the LH process which has a significant activation energy (*11, 20*) and plays a main role in eliminating CO(ad) from the surface as shown later.

3.1.d. Initial CO coverage dependence. The dependence of the transient CO_2 production on the initial CO coverage, θ_{CO}^0, is shown in Fig. 3. The coverage was estimated by flash desorption; the catalyst was cooled to room temperature from 700 K and exposed to CO at a desired pressure for 120 s, and the amount of CO adsorbed during

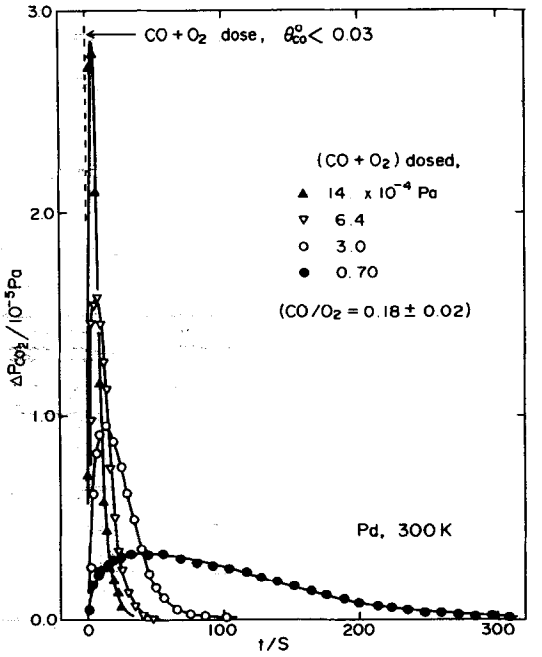

FIG. 2. Variation of the transient CO_2 production generated by the (CO + O_2) pressure jump at $\theta_{CO}^0 <$ 0.03 with pressures of the mixture gas dosed. The apparent total pressures were constant during the transition.

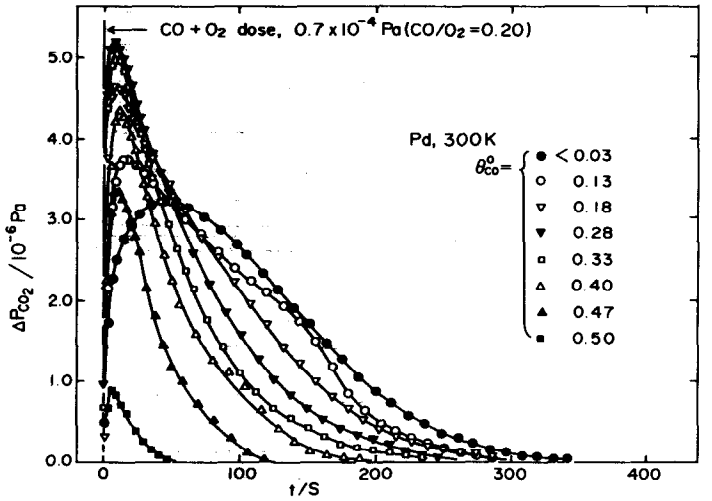

FIG. 3. Variation of the transient CO_2 production with initial CO coverage, θ_{CO}^0.

this period was determined by flash desorption. The coverage was defined as the peak area of CO relative to the maximum area that was obtained by flashing from the steady-state CO flow at room temperature. Afterward the catalyst was exposed to CO in the same manner as before, but in this case the gas mixture was introduced after the leak valve of CO was closed while the CO_2, CO, and O_2 peaks were recorded.

Below $\theta_{CO}^0 = 0.3$ the maximum CO_2 production increased with an increase in θ_{CO}^0 and that position shifted toward small t values. After the maximum in the rate had occurred, the rate decreased almost exponentially with t. Sometimes a small shoulder appeared as seen around 130 s in the case of $\theta_{CO}^0 = 0.13$, but it was not always reproduced. Above $\theta_{CO}^0 = 0.3$ the maximum rate decreased with an increase in θ_{CO}^0. No CO_2 was produced when $\theta_{CO}^0 > 0.5$. The transient isotope tracer method can only be applied on the surface precovered by CO of $\theta_{CO}^0 < 0.5$.

3.1.e. Amounts of adsorbed CO and oxygen in the course of the reaction. The amounts of CO and oxygen adsorbed were determined by flash desorption during the transient CO_2 production at various temperatures. The results at 330 K are shown in Fig. 4. Typical flash desorption spectra of CO and CO_2 are displayed in Figs. 5 and 6. These were generated at a time of t_{dose} after the onset of the transient CO_2 production when the leak valve was closed. The CO_2 peak consists of two parts as seen in Fig. 6a, the first with maximum desorption at 430 K and the second around 500 K. The second disappeared when t_{dose} was large. A similar splitting was observed on Pt (*18*) and Ir (*19*). As long as the gas mixture ($CO/O_2 = 0.26$) was used, no O_2 was desorbed even when the catalyst was heated to 1000 K. All oxygen ad-atoms will react with CO (as seen later, adsorbed CO) and be removed as CO_2. Therefore the amounts of CO and oxygen adsorbed could be estimated from the peak areas of CO and CO_2. The oxygen value was confirmed by CO titration (*4*): during the transient CO_2 production the supply of the gas mixture was terminated and then a relatively large dose of CO was applied. This CO dosage gave a sharp pulse of CO_2. The area gives the amount of O(ad). The results are displayed by open squares in Fig. 4. These are in agreement with the amount of CO_2 desorbed during the falsh desorption described above. The latter is shown by closed triangles. The coverages of CO and oxygen, θ_{CO} and θ_O, were defined as the peak areas (after the correction for the

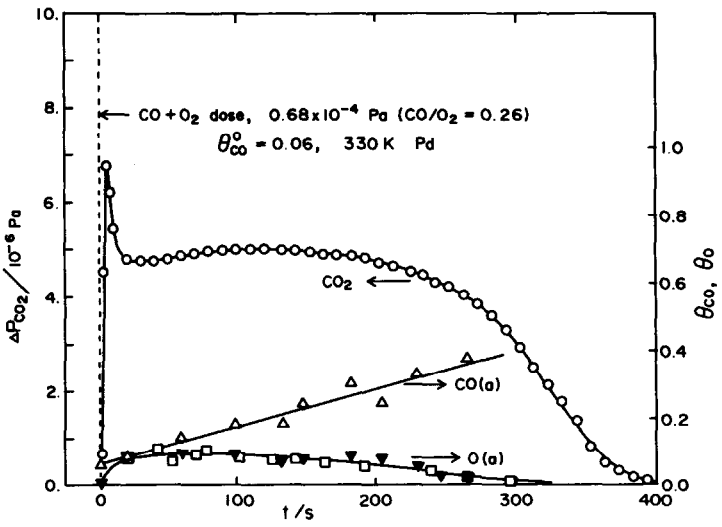

FIG. 4. Variation in the CO_2 pressure and the amounts of CO(ad) and O(ad) during the transient CO_2 production generated by the (CO + O_2) pressure jump. The latter was determined by flash desorption and CO titration. (△) CO(ad) desorbed as CO and CO_2; (▼) O(ad) desorbed as CO_2; and (□) O(ad) determined by CO titration.

sensitivity) of CO plus CO_2 and CO_2 alone relative to the maximum peak area of the CO desorption from room temperature.

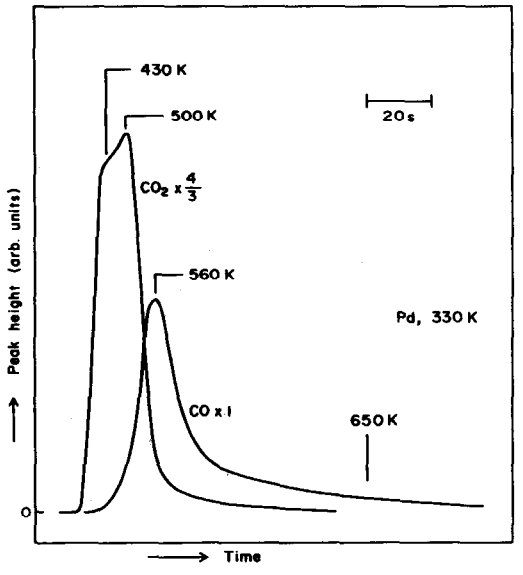

FIG. 5. The CO and CO_2 flash desorption peaks generated at t_{dose} = 98 s after the onset of the transient CO_2 production induced under the same conditions as those shown in Fig. 4. The catalyst was heated quickly after the closure of the leak valve. No O_2 was observed. The final temperature was 1000 K.

The peak temperature of the CO desorption was always higher than that of CO_2 (Fig. 5). This means that CO(ad) is removed as CO_2 through the oxidation reaction rather than CO *via* the thermal desorption. This phenomenon was observed previously by a pressure jump method (*11, 21*) and quite similar to that on Pt (*18*) and Ir (*19*). At higher temperatures and low concentrations of oxygen, the desorption of CO becomes comparable or faster than the formation of CO_2.

The CO coverage increased almost linearly along with the course of the transient CO_2 production, whereas the oxygen coverage showed a maximum and decreased slowly. The CO_2 production showed a sharp pulse in the initial portion when a significant amount of CO was preadsorbed and the reaction temperature was high. The rate of CO_2 production decreased rapidly around 300 s and also the amount of O(ad) became very small. Therefore, the rate is controlled in general by oxygen adsorption in the latter portion of the transient CO_2 production.

3.1.f. Displacement of adsorbed CO by gaseous CO. The displacement of a CO

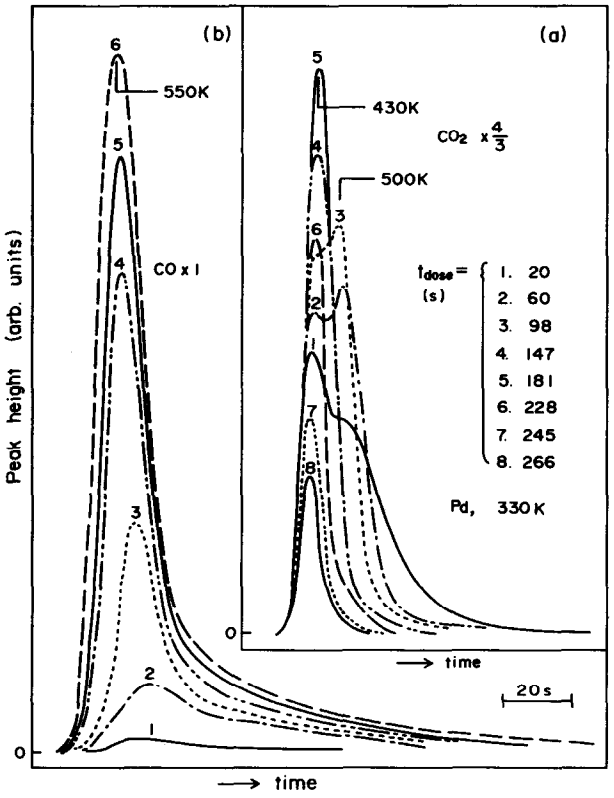

FIG. 6. CO_2 and CO flash desorption peaks generated at different t_{dose} after the onset of the transient CO_2 formation. The experimental conditions were the same as those in Fig. 4.

molecule adsorbed by gaseous CO was studied at various CO pressures and temperatures. The rate over Pd was much larger than that on Pt (*18*) and Ir (*19*). In this experiment the catalyst cooled from 700 K was exposed to ^{12}CO at a desired temperature. After the pressure reached a steady state the ^{12}CO gas was stopped and ^{13}CO (containing the isotope at about 70%) was introduced quickly at the same pressure as before. After desired intervals the catalyst was flashed to 700 K while the partial pressures of ^{12}CO and ^{13}CO were recorded. The amount of the remaining ^{12}CO was determined from the peak area. A typical variation in the partial pressures during the displacement is shown in Fig. 7. The dispalcement was so rapid that the partial pressure of ^{12}CO was still high even while ^{13}CO was dosed and significantly varied. The run with time of the displacement could be represented by a first-order relation:

$$\frac{^{12}CO(ad) - {}^{12}CO(ad)_\infty}{^{12}CO(ad)_0 - {}^{12}CO(ad)_\infty} = \exp(-kt).$$

The symbols $^{12}CO(ad)_0$, $^{12}CO(ad)$, and $^{12}CO(ad)_\infty$ represent the amounts of remaining $^{12}CO(ad)$ at the displacement time $t = 0$, t, and infinite time, respectively. k is a constant showing the displacement rate. The magntiude of $^{12}CO(ad)_\infty$ was estimated by means of an average value of $^{12}CO(g)$ fraction in the gas phase during the displacement. This is an approximate correction for the fact that the isotopic composition in the gas phase varied. The whole amount of CO(ad) was constant during the displacement. The results are shown in Fig. 8.

The half-life of the first-order decay was about 125 s at a CO pressure of 4.3×10^{-5}

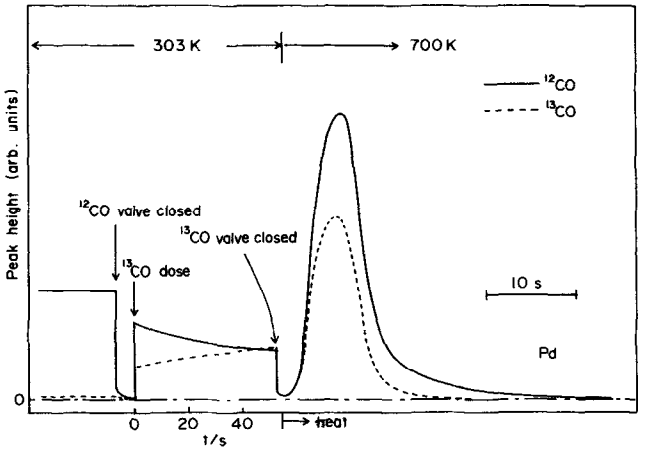

FIG. 7. Variation in the partial pressures during the displacement reaction, $^{12}CO(ad) + {}^{13}CO(g) \rightarrow {}^{12}CO(g) + {}^{13}CO(ad)$. The catlayst was heated quickly after closing the ^{13}CO valve. The total pressure of CO was 8.5×10^{-5} Pa throughout the displacement. The total coverage, $^{12}CO(ad) + {}^{13}CO(ad)$, was constant during the displacement.

Pa and room temperature. It decreased with an increase in the CO pressure to the 0.7th power, and also decreased with an increase in the temperature. The displacement was so rapid even at room temperature that the isotopic carbon monoxide adsorbed would be displaced by gaseous ^{12}CO significantly during the transient isotope tracer experiments. The isotopic composition of the CO_2 produced in the following experiments must be extrapolated to $t = 0$, in order to rule out this influence. In the experiments represented in Fig. 8 (and later with Rh in Fig. 11), the surface was precovered by ^{12}CO and then treated with ^{13}CO.

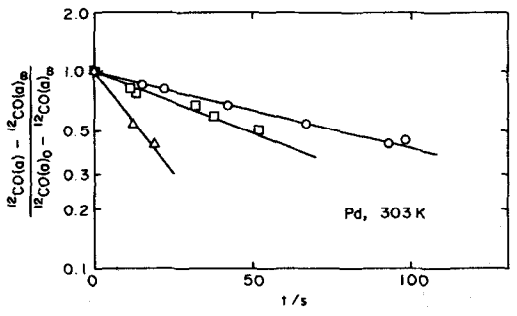

FIG. 8. First-order plots for the isotopic displacement reaction conducted under various pressures. Total pressures ($^{12}CO + {}^{13}CO$): (○) 4.3×10^{-5} Pa; (□) 8.5×10^{-5} Pa; (△) 4.3×10^{-4} Pa.

The reverse sequence was used over Pt (*18*), and Ir (*19*) as reported previously. The sequence $^{12}CO \rightarrow {}^{13}CO$ was selected here in order to minimize the memory effect of carbon 13 remaining in the system.

3.2. Transient CO_2 Production over Rhodium

In this section the results of the preliminary experiments over Rh are briefly summarized. They are quite similar to those over Pd.

3.2.a. Pressure dependence. Figure 9 shows typical results of the transient CO_2 production generated at $\theta_{CO}^0 = 0.08$ with a dosage of the gas mixture ($CO/O_2 = 0.20$) at different pressures. The maximum rate in the CO_2 production on Rh was larger than that on Pd, and the transient production continued for a longer period. This is attributed to the slow adsorption of CO and the rapid removal of CO(ad) through the LH process. The general feature of the dependence of the CO_2 production rate and the total amount of the CO_2 produced on the dosed gas pressure is almost the same as that on Pd.

3.2.b. Initial CO coverage dependence. The dependence on the initial CO coverage is shown in Fig. 10. The CO_2 production

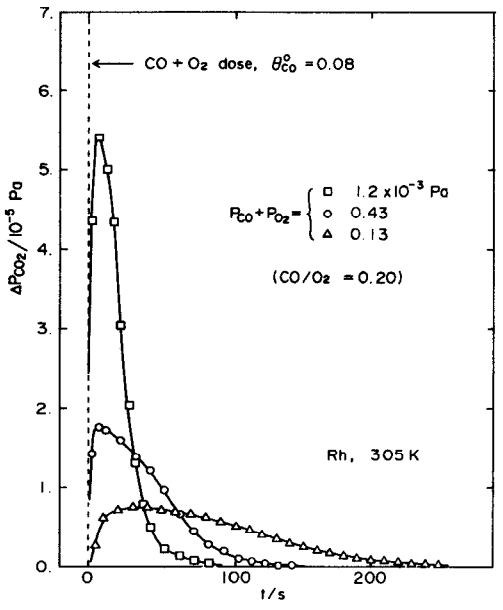

FIG. 9. Variation of the transient CO_2 production generated by the (CO + O_2) pressure jump with pressure of the mixture gas dosed. The apparent total pressures were constant during the transition.

rate (proportional to the CO_2 partial pressure) increased up to the maximum sharply in the initial portion. The maximum rate and also the amount of CO_2 produced became small when θ_{CO}^0 was large. No CO_2 production was observed when $\theta_{CO}^0 >$ about 0.4.

3.2.c. Displacement of $^{12}CO(ad)$ by $^{13}CO(g)$. The results are summarized in Fig. 11. The displacement on Rh was slower than that on Pd. The half-life of the first-order decay was about 320 s at 1.0×10^{-4} Pa and 305 K, which was 4.6 times longer than that on Pd under the same condition. The reciprocal of the half-life increased with the CO pressure to the 0.6th power, and with the catalyst temperature according to an activation energy of 32 kJ $mole^{-1}$. The displacement was slow at relatively high temperatures as compared with on Pd. The transient isotope tracer method can be applied on Rh more easily than on Pd.

3.3. Transient Isotopic CO_2 Production

3.3.a. Over palladium. Figure 12a shows the variation of the partial pressures of $^{13}CO_2$, $^{12}CO_2$, ^{13}CO, ^{12}CO, and O_2 during the transient isotopic CO_2 production. That production was generated by a dosage of a gas mixture of ^{12}CO and O_2 at an apparent total pressure of 0.7×10^{-4} Pa to the surface precovered by carbon monoxide of $\theta_{CO}^0 = 0.22$ and the isotope ratio $^{13}CO(ad)/^{12}CO(ad) = 1.9 \pm 0.1$. The initial CO coverage was determined in the same way as before and the isotopic ratio from the partial pressures of ^{13}CO and ^{12}CO dosed before the transient production. During the transient experiments gaseous ^{13}CO was observed in appreciable amounts but it was

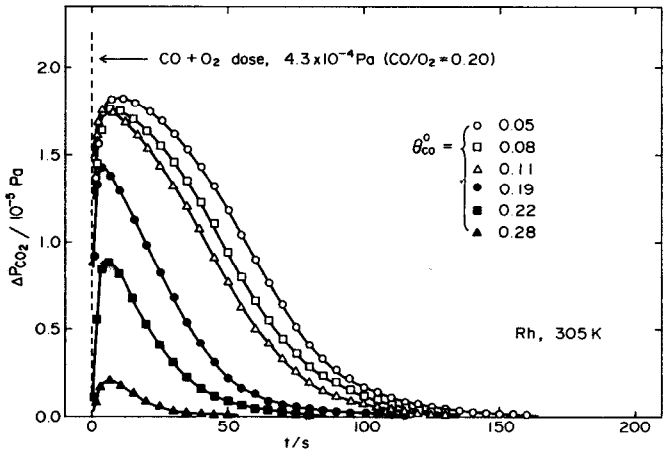

FIG. 10. Variation of the transient CO_2 production with initial CO coverage.

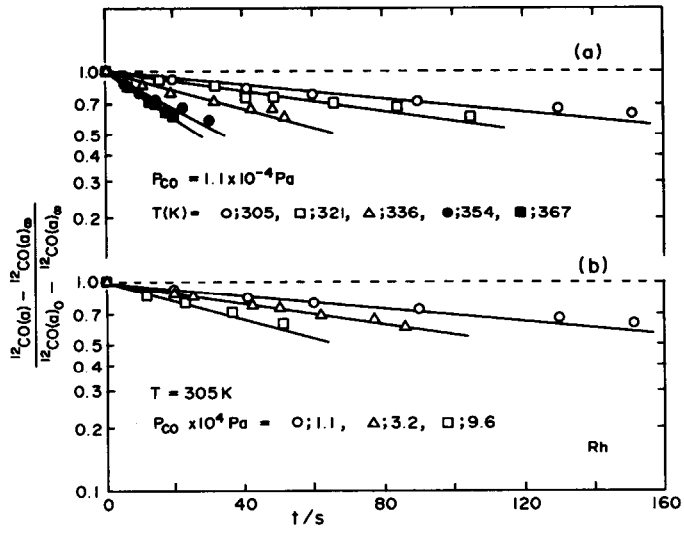

FIG. 11. First-order plots for the isotopic displacement reaction over Rh conducted at various temperatures (a) and under various pressures (b).

less than 6% of that of ^{12}CO. $^{13}CO_2$ was produced significantly in the initial portion but decreased rapidly. On the other hand $^{12}CO_2$ showed a peak and then a small shoulder around 100 s. The $^{13}CO_2$ + $^{12}CO_2$ sum agreed with the $^{12}CO_2$ production induced at the same θ_{CO}^0 in the pure ^{12}CO system.

In order to estimate the ratio of $^{13}CO_2$ to $^{12}CO_2$ at $t = 0$, the logarithm of the ratio of $^{13}CO_2$ to $^{12}CO_2$ was plotted against the dose time and extrapolated to $t = 0$. Such extrapolation was suitable since the partial pressures of $^{12}CO_2$ and $^{13}CO_2$ did not vary monotonically in the initial portion, whereas the ratio decreased almost exponentially as seen in Fig. 12b. The initial ratio extrapolated in this manner, 1.8 ± 0.2,

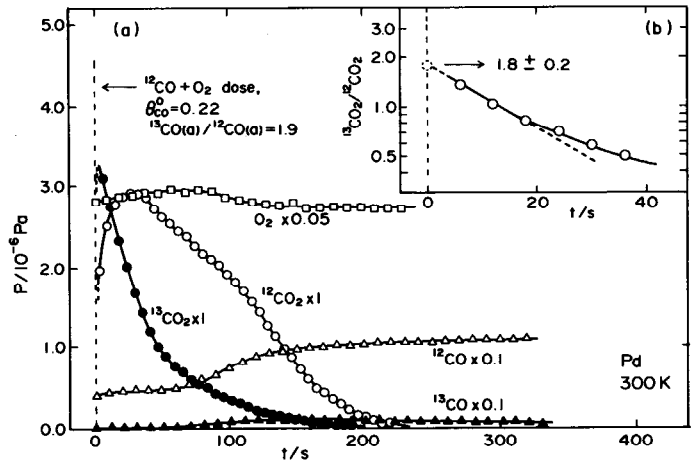

FIG. 12. (a) Variation in the partial pressures of ^{12}CO, ^{13}CO, O_2, $^{12}CO_2$, and $^{13}CO_2$ during a transient isotopic carbon dioxide production induced at an apparent total pressure of 0.7 × 10^{-4} Pa. The surface was precovered by carbon monoxide containing ^{13}CO at the ratio $^{13}CO(ad)/^{12}CO(ad)$ = 1.9. (b) Estimation of the initial ratio of $^{13}CO_2$ to $^{12}CO_2$. The ratio determined is shown by the dotted circle.

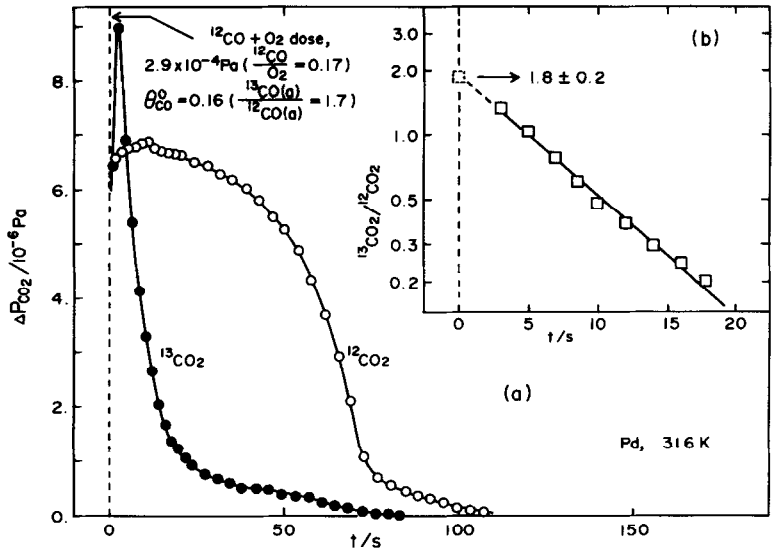

FIG. 13. (a) A transient isotopic carbon dioxide production induced at an apparent pressure of 2.9×10^{-4} Pa. The surface was precovered by carbon monoxide at the ratio $^{13}CO(ad)/^{12}CO(ad) = 1.7$. (b) Estimation of the initial ratio of $^{13}CO_2$ to $^{12}CO_2$.

as designated by the dotted circle in Fig. 12b, equaled that of $^{13}CO(ad)$ to $^{12}CO(ad)$ in the carbon monoxide preadsorbed, 1.9 ± 0.1, within the margin of experimental errors. The isotope ratio in the carbon dioxide decreased rapidly with the time, since the isotope ratio in the carbon monoxide adsorbed decreased through the adsorption of ^{12}CO and the displacement by $^{12}CO(g)$. Figures 13 and 14 show other transient isotopic oxidation rates at two different high pressures, 2.9×10^{-4} Pa and 1.1×10^{-3}

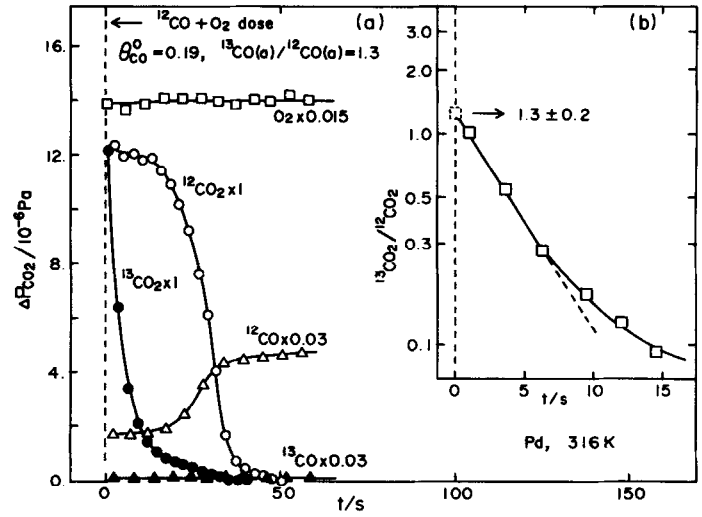

FIG. 14. (a) Variation in the partial pressures of ^{12}CO, ^{13}CO, O_2, $^{12}CO_2$, and $^{13}CO_2$ during a transient isotopic carbon dioxide production induced at an apparent total pressure of 1.1×10^{-3} Pa. The surface was precovered by carbon monoxide at the ratio $^{13}CO(ad)/^{12}CO(ad) = 1.3$. (b) Estimation of the initial ratio of $^{13}CO_2$ to $^{12}CO_2$.

Pa. The rate of the CO_2 production ($^{13}CO_2$ + $^{12}CO_2$) increased with pressure of the gas mixture dosed, however, the initial ratio of $^{13}CO_2$ to $^{12}CO_2$ still equaled that of ^{13}CO(ad) to ^{12}CO(ad) in the carbon monoxide preadsorbed. The dotted squares in Figs. 13b and 14b represent the initial isotope ratios in the carbon dioxide extrapolated to $t = 0$. The equality between the ratio of $^{13}CO_2$ to $^{12}CO_2$ in the carbon dioxide at $t = 0$ and that of ^{13}CO(ad) to ^{12}CO(ad) in the carbon monoxide preadsorbed held true for the coverage range studied, $\theta_{CO}^0 = 0.05$–0.50, and the mixture gas pressure range dosed, 3.0×10^{-5}–1.1×10^{-3} Pa. Accordingly it can be concluded that all CO molecules oxidized to CO_2 from the chemisorption state, i.e., the LH process is operative. In the case of the ER process the isotope ratio in CO_2 should equal that in gaseous CO. No contribution from the latter was observed.

3.3.b. Over rhodium. The results over Rh are shown in Fig. 15. A significant production of $^{13}CO_2$ was observed as well as that of $^{12}CO_2$. The variation in the partial pressures of ^{12}CO, ^{13}CO, and O_2 was essentially the same as that over Pd. The maximum CO_2 production was large and the rate of $^{13}CO_2$ and $^{12}CO_2$ production decreased rapidly, as the pressure of the gas mixture dosed was relatively high (1.2×10^{-3} Pa). The initial isotope ratio in the carbon dioxide was extrapolated in the same way as before. The ratio determined, 1.05 ± 0.1, is shown by the dotted circle in Fig. 15b. It agreed well with the initial isotope ratio in the carbon monoxide preadsorbed. The equality between the initial ratio of $^{13}CO_2$ to $^{12}CO_2$ and that of ^{13}CO(ad) to ^{12}CO(ad) held true for all of the conditions studied, $\theta_{CO}^0 = 0.06$–0.40., and the mixture gas pressure, 3.0×10^{-5}–2.0×10^{-3} Pa. The LH process can be concluded also over rhodium. No contribution from the ER process was observed.

3.3.c. Kinetics of the Langmuir–Hinshelwood process and possibility of the Eley—Rideal process. Engel and Ertl analyzed the kinetics of the LH process over the Pd(111) plane at high temperatures using a modulated molecular beam method. Their results showed that the reaction was fast with a second-order rate constant, $k = 1.1 \times 10^{-11}$ exp(-104 kJ/RT) molecules^{-1} cm^2 sec^{-1}. For moderate CO coverages, a

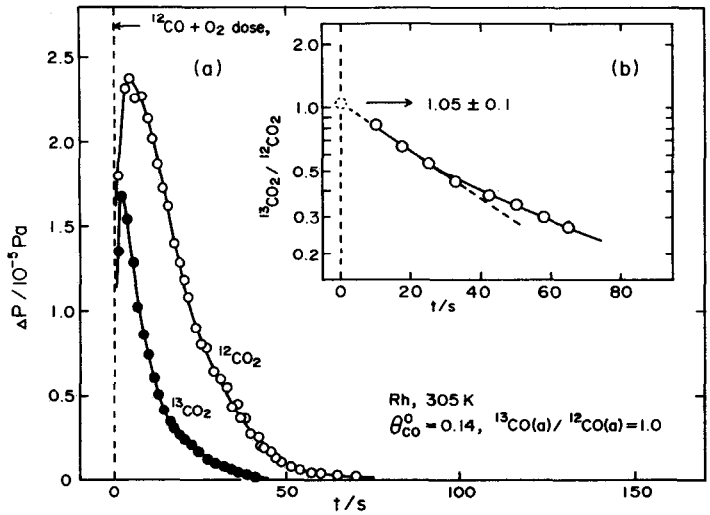

FIG. 15. (a) Variation in the partial pressures of $^{13}CO_2$ and $^{12}CO_2$ during a transient isotopic carbon dioxide production on rhodium. The Rh surface was precovered by carbon monoxide containing ^{13}CO at the ratio $^{13}CO(ad)/^{12}CO(ad) = 1.0$. The total pressure of the mixture gas dosed was 1.2×10^{-3} Pa and the ratio $CO/O_2 = 0.20$. (b) Estimation of the initial ratio of $^{13}CO_2$ to $^{12}CO_2$.

rearrangement of the oxygen ad-layer takes place resulting in a reduction of the activation energy to 58.4 kJ mole^{-1}. In the latter case k is estimated to $1.0 \times 10^{-7} \exp(-58.4$ kJ/RT) molecules^{-1} cm^2 sec^{-1} from their results. Although a simple kinetic expression for the rate constant is not valid over a wide range of temperature and the CO and oxygen coverages, the rate of the LH process will be estimated roughly by using the rate constant for the moderate coverage. Assuming the catalyst used here consists predominantly of (111) oriented crystallites and that the saturation concentrations of CO and oxygen are approximately 1×10^{15} molecules cm^{-2} and 5.1×10^{14} atoms cm^{-2} (*14, 17*), respectively, the maximum rate of the LH process at room temperature is estimated to be 9.3×10^{11} molecules sec^{-1} cm^{-2} for $\theta_{CO} = \theta_O = 0.5$. This rate can only produce a CO_2 pressure of 8×10^{-7} Pa in the vacuum system used here. The actual coverages observed were smaller than a half. The rate actually observed in this process, however, could produce a CO_2 pressure of 2.4×10^{-5} Pa in the case of the experiment shown in Fig. 14, and further it could increase with an increase in the pressure of the gas mixture dosed. This large discrepancy suggests that the rate constant of the LH process strongly depends on the structure of the adsorbed layer; the activation energy is probably reduced to much less than 58.4 kJ mole^{-1} and/or the preexponential factor becomes large, being due to compression of the adsorbed layer. The estimation described above is concerned with Pd. The LH process is somewhat more rapid on Rh than Pd. Therefore the same discussion is possible also on Rh.

On the other hand, the ER process over Pd was thought to be very rapid with unity reaction probability of incident CO on the surface covered by oxygen (*4*). Assuming that the reaction probability is one-tenth on the surface covered by oxygen at the coverage = 0.1 (see Fig. 4) and introducing CO at a pressure of 6×10^{-5} Pa (4.5×10^{-7} Torr), which is close to the initial CO pressure in the experiments shown in Figs. 14 and 15, the rate of the ER process is estimated to be 1.7×10^{13} molecules sec^{-1} cm^{-2}. This rate of the CO_2 formation can produce a CO_2 pressure of 1.5×10^{-5} Pa in this vacuum system. Such a CO_2 formation through the ER process was not observed experimentally. In a previous paper concerning CO oxidation over Pt (*9*), we discussed the reasons why the contribution from the ER process was not observed by the tracer method although it had been thought to be much faster than the LH process around room temperature; the kinetics of the ER process was studied through analysis of the transient CO_2 production from an interaction of gaseous CO with the surface fully covered by oxygen. The rate of the CO_2 production observed was extremely large. Therefore, even if the incident CO must stay, but remain for a short duration in the chemisorption state before being oxidized (i.e., the LH process), the observed kinetics will behave as if the reaction took place *via* the ER process, i.e., rapid CO_2 production and no activation energy. The fact is that the rapid CO_2 production takes place simply through the LH process. The same discussion is possible also on Pd and Rh, since these metals precovered by oxygen interact rapidly with gaseous CO to form CO_2 (*1, 3, 4, 8, 13*).

In the case of Pt and Ir, the ratio of $^{13}CO_2$ to $^{12}CO_2$ in the CO_2 produced decreased more rapidly than the average ratio of ^{13}CO(ad) to ^{12}CO(ad) in the adsorbed layer. This means that the later CO adsorbs, the higher the reactivity is. Such heterogeneity in the reactivity of CO(ad) could not be examined over Pd and Rh, because the displacement of ^{13}CO(ad) by ^{12}CO(g) was so rapid that the amount of ^{13}CO(ad) removed as ^{13}CO(g) from the surface was not negligible as compared with that of ^{13}CO(ad) removed as $^{13}CO_2$(g). The experiments for this purpose should be conducted at low temperatures to reduce the displacement rate.

Finally the conditions for the transient isotope tracer experiments will be compared with those for the kinetic experiments in a steady state (*8, 22*). Kinetic studies on the CO oxidation in a steady state have shown that the inhibition region by carbon monoxide appears for $P_{CO} > P_{O_2}$ and is extended with a decrease of the temperature (*22*). In this region the surface is covered with carbon monoxide at an equilibrium level with gaseous CO (*21*), whereas the amount of adsorbed oxygen is negligible (*5*). Kinetically the rate is controlled by the dissociative adsorption of oxygen (*8, 22*). The noninhibition region is very narrow at room temperature. In the experiments described in this paper, the surface was always precovered by carbon monoxide. The amount of adsorbed oxygen during the transient experiments increased initially and decreased slowly, but it was always small. This reaction environment consists of CO and O_2 in the gas phase, and also CO ad-molecules and a small amount of oxygen ad-atoms in the adsorbed layer. These conditions are quite similar to those observed in the CO inhibition region at a steady state. However, when the initial CO coverage was small, the CO_2 formation rate in the initial portion increased with an increase in the coverage. This fact means that some parts of the conditions used here correspond to the noninhibition region. One of the purposes of this paper is to distinguish which CO molecule in the gas phase or adsorbed layer reacts preferentially with oxygen ad-atoms under the conditions where each CO molecule can partcipate simultaneously in the oxidation especially at low temperatures. At high temperatures the LH process can be predicted to predominate to a greater extent, since the activation energy is larger than that of the ER process. At times the LH process was concluded in the reaction system which consisted of the adsorbed CO and only O_2 in the gas phase (*23*). Such experiments, however, cannot exclude the contribution from the ER process.

ACKNOWLEDGMENTS

This work was supported in part by the Matsunaga Science Foundation and by Grant-in-Aid 343001 for scientific research from the Ministry of Education.

REFERENCES

1. Ertl, G., and Rau, P., *Surface Sci.* **15**, 443 (1969).
2. Bonzel, H. P., and Ku, R., *Surface Sci.* **33**, 91 (1972).
3. Ertl, G., and Koch, J., *in* "Proc. 5th Int. Congr. on Catal." (J. W. Hightower, Ed.), p. 969. North-Holland, Amsterdam, 1973.
4. Matsushima, T., and White, J. M., *J. Catal.* **39**, 265 (1975).
5. Matsushima, T., and White, J. M., *Surface Sci.* **67**, 122 (1977).
6. Matsushima T., Almy, D. B., and White, J. M., *Surface Sci.* **67**, 89 (1977).
7. White, J. M., and Golchet, A., *J. Chem. Phys.* **66**, 5744 (1977).
8. Campbell, C. T., and White, J. M., *J. Catal.* **54**, 289 (1978).
9. Matsushima, T., *J. Catal.* **55**, 337 (1978).
10. Bonzel, H. P., and Burton, J. J., *Surface Sci.* **52**, 223 (1975).
11. Matsushima, T., and White, J. M., *J. Catal.* **40**, 334 (1975).
12. Campbell, C. T., Shi, S. K., and White, J. M., *Appl. Surface Sci.* **2**, 382 (1979).
13. Campbell, C. T., Shi, S. K., and White, J. M., *J. Vac. Sci. Technol.* **16**, 605 (1979); *J. Phys. Chem.* **83**, 2255 (1979).
14. Conrad, H., Ertl, G., and Küppers, J., *Surface Sci.* **76**, 323 (1978).
15. Engel, T., and Ertl, G., *in* "Proc. 7th Int. Vac. Congr. and 3rd Int. Conf. Solid Surfaces (Vienna, 1977)," p. 1365.
16. Engel, T., and Ertl, G., *Chem. Phys. Lett.* **54**, 95 (1978).
17. Engel, T., and Ertl, G., *J. Chem. Phys.* **69**, 1267 (1978).
18. Matsushima, T., *Surface Sci.* **79**, 63 (1979).
19. Matsushima, T., *Surface Sci.* **87**, 665 (1979).
20. Ertl, G., and Neumann, M., *Z. Phys. Chem. N.F.* **90**, 127 (1974).
21. Matsushima, T., Mussett, C. J., and White, J. M., *J. Catal.* **41**, 397 (1976).
22. Matsushima, T., Almy, D. B., Foyt, D. C., Close, J. S., and White, J. M., *J. Catal.* **39**, 277 (1975).
23. Shigeishi, R. A., and King, D. A., *Surface Sci.* **75**, L397 (1978).